



Published in final edited form as:

Phys Rev E Stat Nonlin Soft Matter Phys. 2009 July ; 80(1 0 1): 011906.

Discretization of the Induced-Charge Boundary Integral Equation

Jaydeep P. Bardhan^{1,2,*}, Robert S. Eisenberg^{2,3}, and Dirk Gillespie²

¹Biosciences Division Argonne National Laboratory, Argonne IL, USA

²Department of Molecular Biophysics and Physiology Rush University Medical Center, Chicago IL, USA

³Mathematics and Computer Science Division Argonne National Laboratory, Argonne IL, USA

Abstract

Boundary-element methods (BEM) for solving integral equations numerically have been used in many fields to compute the induced charges at dielectric boundaries. In this paper, we consider a more accurate implementation of BEM in the context of ions in aqueous solution near proteins, but our results are applicable more generally. The ions that modulate protein function are often within a few Angstroms of the protein, which leads to the significant accumulation of polarization charge at the protein/solvent interface. Computing the induced charge accurately and quickly poses a numerical challenge in solving a popular integral equation using BEM. In particular, the accuracy of simulations can depend strongly on seemingly minor details of how the entries of the BEM matrix are calculated. We demonstrate that when the dielectric interface is discretized into flat tiles, the qualocation method of Tausch, Wang, and White (*IEEE. Trans. Comput.-Aided Des.* **20**:1398, 2001) to compute the BEM matrix elements is always more accurate than the traditional centroid collocation method. Qualocation is no more expensive to implement than collocation and can save significant computational time by reducing the number of boundary elements needed to discretize the dielectric interfaces.

Keywords

electrostatics; ion permeation; solvation; boundary-integral equation; channel protein boundary-element method

1. INTRODUCTION

Protein function almost always depends on the ions in the surrounding solution. In a very real sense, ionic solutions are the liquid of life. Ions direct the biological function of cells and tissues by interacting with proteins—acting as messengers that control channel proteins in cell membranes, binding to proteins in membranes or in the cytoplasm, or directing enzymes to perform chemical reactions when concentrations of messengers (often Ca^{2+}) reach threshold levels (see, for instance, [1]). Furthermore, gradients of ion concentrations—usually Na^+ —are the energy supply for an enormous range of biological functions. These dependencies motivate experimental studies of proteins that commonly employ many types of ions over a wide range of concentrations, in some cases spanning as many as five orders of magnitude. Theoretical studies of protein function must therefore be capable of rapidly and accurately simulating proteins in a comparably wide range of ionic solutions.

*jbardhan@alum.mit.edu.

The ions that interact with proteins, enzymes, and channels can be within a few Angstroms of the protein–solvent boundaries where dielectric properties change, so polarization charge accumulates in significant amounts. The strong electric fields produced by these induced charges are vital for accurate modeling of channel-protein selectivity [2, 3], and are likely to be important for protein function in general [4]. Unfortunately, because biological systems are often controlled by messengers at a concentration of $\sim 10^{-7}$ M in ~ 55 M water, fully atomistic simulations (that is, simulations that include explicit water molecules) require at least 10^9 atoms to even approximately study these solutions—well beyond the reach of typical molecular-modeling software, even on supercomputers. For this reason, ionic solutions are often described using implicit solvent with explicit ions, using what is known as the primitive model [5]. The primitive model of ionic solutions treats the solvent as a homogeneous dielectric, with explicit, mobile point charges to model the ions. Such reduced models of ionic solutions appear to be an important approach for investigating the dependence of protein function on ionic conditions, and have been applied successfully to a variety of problems (*e.g.*, [6–8]). Dilute ionic solutions are also commonly studied using Poisson–Boltzmann (PB) theory [9–22], with reasonable agreement for the energetics between PB theory and primitive-model Monte-Carlo simulations, for sufficiently low concentrations of monovalent salts [23–26].

Reduced models of proteins and ions often treat the electrostatic interactions using macroscopic continuum theory, treating the protein interior as a homogeneous medium with low dielectric constant, possibly with permanent (*i.e.*, fixed) charges, and the solvent region as a uniform high-dielectric medium with mobile ions. By solving Poisson’s equation with spatially varying dielectric constant, one obtains the electrostatic potential throughout space [27]. A wide range of numerical simulation methodologies, most often the finite-difference and finite-element methods, have been proposed [9, 16, 28–30] to solve this elliptic partial-differential equation (PDE).

An alternative viewpoint, the implementation details of which form the primary argument of this paper, leads to the description of the problem via a boundary-integral equation rather than a PDE [12, 31, 32]. The ion and protein charges create an electric field, which leads to the development of an induced polarization charge at the dielectric boundaries. Efficient and accurate computation of the polarization charge at these boundaries is an essential part of a theory or simulation of these systems. Levitt introduced one of the first boundary-integral equations for molecular electrostatics, in an analytical study of dielectric effects in ion-channel proteins [33]. Jordan and collaborators later made significant advances in applying this methodology and solving the integral equation, again analytically [34, 35]. These studies employed particularly simple geometries, however, and generally speaking the integral equation must be solved numerically. More recent studies of channel proteins have employed boundary-element methods (BEM) for this purpose [3, 36, 37]. Interestingly, the same integral equation has a long, apparently independent history in quantum chemistry (*e.g.*, Miertus *et al.* [38, 39]) where it is called the polarizable continuum model (PCM) for *ab initio* calculations (see, for example, [40]). Shaw also derived this integral equation for studying proteins [32], and Shaw and Zauhar established much of the early boundary-element literature for simulating protein electrostatics [41–44].

Unfortunately, BEM are generally more challenging to implement than their PDE-simulation counterparts such as the finite-difference and finite-element methods [9, 16, 17, 28]. Three challenges are quite well known [22]. First, the solute–solvent boundaries can be extremely complicated if one uses an atomistically detailed boundary representation [45]. Second, it can be challenging to calculate the diagonal and near-diagonal entries of the BEM matrix because these entries require the evaluation of singular or near-singular integrals (that is, integrals whose value is well defined even though the integrand goes to infinity

somewhere in the domain of integration, or in the near singular case that the integrand is very sharply peaked). Third, it can be time and memory intensive to form the dense BEM matrix, and even more time intensive to calculate its LU factorization. Fast methods for BEM simulations, which employ matrix-sparsification techniques such as the fast-multipole method [46, 47], alleviate this situation for many, but not all, investigations of proteins in ionic solution [3, 26].

In the present paper, we consider a different challenge for BEM implementation. The accuracy of simulations can depend very strongly on the details of how the entries of the BEM matrix are calculated. As we demonstrate, the details of the matrix-entry computation, which can seem relatively unimportant compared to the well-known challenges already mentioned, can significantly degrade accuracy even when one uses more and more expensive computational methods (*i.e.*, higher-resolution simulations). Fortunately, the challenge appears to have been largely resolved by the work of Tausch, Wang, and White [48], who presented an alternative discretization, called *qualocation*, for the integral formulation known as the apparent-surface-charge (ASC) method [32], which is also called the induced-charge computation (ICC) [3]. Their study originated in an effort to develop a purely second-kind integral-equation method for estimating parasitic capacitances between conductors embedded in a homogeneous dielectric. Greengard and Lee have also analyzed this integral-equation formulation [49]. The qualocation approach to discretization is equally useful for the ICC in addressing the mixed-dielectric Poisson problem in protein electrostatics [50, 51].

However, whereas the earlier work focused on the effect on the energetics due to permanent charge in the protein, in the present paper we focus our attention on mobile ions in solution, and the effect that discretization has on the energetics of these mobile ions. Our study is directed in particular towards application of enormous biological importance [52, 53]—ions in channels—and present two methods to solve the ICC integral-equation. Although both methods, called collocation and qualocation, use comparably simple numerical integration schemes, the qualocation approach introduced by Tausch *et al.* [48] is much better suited for the ICC equation (Equation (1) below), offering reductions in computational time because the dielectric boundary can be discretized using fewer elements. Our results suggest that the qualocation approach is even more valuable for mobile charges in the high-dielectric solvent than it is for permanent charges situated in low-dielectric regions.

The following section presents our mathematical model for continuum electrostatics, and boundary-element methods as a means to numerically solve integral equation formulations of the mathematical model. Section 3 illustrates the importance of using careful discretization approaches, using the analytically solvable case of a charge in a dielectric sphere, embedded in a homogeneous medium with a different dielectric constant. Section 4 summarizes the paper, discusses the implications of the numerical results, and highlights areas for future work.

2. THEORY

2.1. Continuum Electrostatic Model

We describe the interior of a protein molecule as a dielectric with uniform low permittivity ϵ_1 and the exterior solvent region as a dielectric with uniform high permittivity ϵ_2 . The boundary β separating these two regions is impenetrable to ions or water. At β both the electrostatic potential and the normal flux are continuous. The system contains only a set of discrete point charges with values independent of the electric field, the i th of which has value q_i and is located at r_i ; we refer to such charges as *fixed* charges. There are no continuous densities of charge that exist independent of the electric field, and the only

charge that depends on the electric field is the polarization charge induced on the boundary β . This mixed-dielectric problem can be transformed into a boundary-integral equation that is known variously as the induced-charge computation (ICC) method, the apparent-surface-charge (ASC) formulation, and the polarizable-continuum model (PCM) [3, 32, 33, 38, 54, 55]. We call it the ICC method and write the electrostatic integral equation as

$$h(\mathbf{s}) + \frac{\Delta\epsilon(\mathbf{s})}{4\pi\bar{\epsilon}(\mathbf{s})} \mathbf{n}(\mathbf{s}) \cdot \int_{\beta} \frac{\mathbf{s}-\mathbf{s}'}{|\mathbf{s}-\mathbf{s}'|^3} h(\mathbf{s}') d\mathbf{s}' = -\frac{\Delta\epsilon(\mathbf{s})}{4\pi\bar{\epsilon}(\mathbf{s})} \mathbf{n}(\mathbf{s}) \cdot \sum_k \frac{q_k}{\epsilon(\mathbf{r}_k)} \frac{\mathbf{s}-\mathbf{r}_k}{|\mathbf{s}-\mathbf{r}_k|^3}, \quad (1)$$

where \mathbf{s} is a point on β , $h(\mathbf{s})$ is the induced charge at the dielectric boundary, $\epsilon(\mathbf{r}_k)$ is the dielectric constant at the point \mathbf{r}_k , $\mathbf{n}(\mathbf{s})$ denotes the outward normal (that is, pointing outward from the protein into the interior of the pore) at \mathbf{s} ,

$$\Delta\epsilon(\mathbf{s}) = \epsilon_2 - \epsilon_1, \quad (2)$$

and

$$\bar{\epsilon}(\mathbf{s}) = \frac{1}{2}(\epsilon_1(\mathbf{s}^-) + \epsilon_2(\mathbf{s}^+)), \quad (3)$$

with

$$\mathbf{s}^{\pm} = \mathbf{s} \pm \delta \mathbf{n}(\mathbf{s}) \quad (4)$$

for sufficiently small δ . The integrals in Equation (1) are taken to be the Cauchy principal value integrals [50, 54]. Having solved for the distribution of induced charge on the boundary, the electrostatic *reaction potential* induced at a point \mathbf{r}_0 by the surface charge density on the boundary β is

$$\phi^R(\mathbf{r}_0) = \int_{\beta} \frac{h(\mathbf{s})}{4\pi\epsilon_0|\mathbf{r}_0-\mathbf{s}|} d\mathbf{s}. \quad (5)$$

2.2. Boundary-Element Methods

The boundary-element method is a numerical technique for finding approximate solutions to boundary integral equations such as Equation (1). Introductions to boundary-element methods may be found in several texts on integral equations [31, 56, 57] as well as in the literature [58]. One can define a representation of the unknown induced surface charge $h(\mathbf{s})$ as a weighted sum of *basis functions* defined on the boundary β , or on an approximation to the boundary, $\hat{\beta}$. For general surfaces, it is typically easiest to define a surface approximation and then use basis functions that are easily defined on the approximate surface. Here, we approximate the surface β as a set of N planar triangles $\beta_1, \beta_2, \dots, \beta_N$ and define piecewise-constant basis functions $\chi_1(\mathbf{s}), \dots, \chi_N(\mathbf{s})$ such that $\chi_i(\mathbf{s}) = 1$ if \mathbf{s} is on β_i and 0 otherwise. The approximate solution $\hat{h}(\mathbf{s})$ is then represented as the weighted combination

$$\widehat{h}(\mathbf{s}) = \sum_{i=1}^N h_i \chi_i(\mathbf{s}), \quad (6)$$

where the weights h_i are yet to be determined.

Boundary-element methods ensure that the chosen approximate solution is, in some sense, as close as possible to the exact solution by forcing the *residual*

$$R(\mathbf{s}) = f(\mathbf{s}) - (\mathcal{I} + \widehat{\varepsilon}(\mathbf{s})\mathcal{K})\widehat{h}(\mathbf{s}), \quad (7)$$

to satisfy a set of N linear constraints, giving a matrix equation $Ah = b$ in which the matrix A is square with dimension N . In Equation (7), $f(\mathbf{s})$ is the right-hand side of Equation (1), the identity operator is denoted by \mathcal{I} , $\widehat{\varepsilon}(\mathbf{s}) = \Delta \varepsilon(\mathbf{s})/\varepsilon(\mathbf{s})$, and the normal electric-field operator is denoted by \mathcal{K} . The entries of the BEM matrix A and the right-hand side vector b are defined in part by the kinds of constraints imposed to form the matrix equation.

Galerkin boundary-element methods force the residual to be orthogonal to the basis functions. Thus, for piecewise constant basis functions, the N Galerkin conditions are defined by

$$\int_{\beta_i} R(\mathbf{s}) d\mathbf{s} = 0 \quad (8)$$

where β_i denotes the i th panel, and substituting the residual definition from Eq. (7) into Eq. (8), we have, for each boundary element i ,

$$0 = \int_{\beta_i} \left([\mathcal{I} + \widehat{\varepsilon}(\mathbf{s})\mathcal{K}] \widehat{h}(\mathbf{s}) - f(\mathbf{s}) \right) d\mathbf{s}. \quad (9)$$

Because $\chi_j(\mathbf{s}) = 0$ if $\mathbf{s} \in \beta_j, j \neq i$, we can expand the first term and write

$$0 = \int_{\beta_i} \left(h_i + \widehat{\varepsilon}(\mathbf{s})\mathcal{K} \widehat{h}(\mathbf{s}) - f(\mathbf{s}) \right) d\mathbf{s}. \quad (10)$$

Expanding the integral operator $\mathcal{K}(\mathbf{s}; \mathbf{s}')$ gives

$$0 = \int_{\beta_i} \left(\left[h_i + \widehat{\varepsilon}(\mathbf{s}) \sum_{j=1}^N h_j \int_{\beta_j} \left(\mathbf{n}(\mathbf{s}) \cdot \frac{\mathbf{s} - \mathbf{s}'}{4\pi|\mathbf{s} - \mathbf{s}'|^3} \right) d\mathbf{s}' \right] - f(\mathbf{s}) \right) d\mathbf{s}. \quad (11)$$

The BEM matrix entries thus take the form

$$A_{ij} = \int_{\beta_i} \left(\delta_{ij} + \int_{\beta_j} \left(\frac{\Delta \varepsilon}{4\pi \varepsilon} \frac{\mathbf{n}(\mathbf{s}) \cdot (\mathbf{s} - \mathbf{s}')}{|\mathbf{s} - \mathbf{s}'|^3} \right) d\mathbf{s}' \right) d\mathbf{s}, \quad (12)$$

where δ_{ij} is the Kronecker delta function. The right-hand side entries are defined by

$$b_i = - \int_{\beta_i} \left(\frac{\Delta \varepsilon(\mathbf{s})}{4\pi \bar{\varepsilon}(\mathbf{s})} \sum_k \frac{q_k}{\varepsilon(\mathbf{r}_k)} \frac{\mathbf{n}(\mathbf{s}) \cdot (\mathbf{s} - \mathbf{r}_k)}{|\mathbf{s} - \mathbf{r}_k|^3} \right) d\mathbf{s}. \quad (13)$$

2.3. The Centroid-Collocation Discretization

Analytical expressions for the double integrals in Equation (12) exist only for very specialized geometries [59]. Thus, the matrix entries in a Galerkin method must generally be calculated numerically, and are expensive to compute. However, the centroid-collocation discretization is much faster, and in many cases is accurate enough. In centroid collocation, one forces the residual to be zero at the boundary-element centroids—in other words, Equation (7) is forced to be exactly satisfied at those points [31]. The collocation approach is therefore suitable when the residual varies slowly over each boundary element. The right-hand side vector b in the collocation discretization of the ICC has entries

$$b_i = - \frac{\Delta \varepsilon(\mathbf{s}_i)}{4\pi \bar{\varepsilon}(\mathbf{s}_i)} \sum_k \frac{q_k}{\varepsilon(\mathbf{r}_k)} \frac{\mathbf{s}_i - \mathbf{r}_k}{|\mathbf{s}_i - \mathbf{r}_k|^3} \cdot \mathbf{n}(\mathbf{s}_i) \quad (14)$$

and the matrix A has entries

$$A_{ij} = \delta_{ij} + \frac{\Delta \varepsilon(\mathbf{s}_i)}{4\pi \bar{\varepsilon}(\mathbf{s}_i)} \int_{\beta_j} \frac{(\mathbf{s}_i - \mathbf{s}') \cdot \mathbf{n}(\mathbf{s}_i)}{|\mathbf{s}_i - \mathbf{s}'|^3} d\mathbf{s}'. \quad (15)$$

If one-point quadrature is used to approximate the integrals over β_j in Equations (12) and (13), one obtains a row-scaled version of the centroid-collocation linear system. This can be seen by comparing the matrix entries in Equations (12) and (15) and the right-hand-side entries in Equations (13) and (14); the row-scaling factors are the boundary-element areas defined by

$$a_i = \int_{\beta_i} d\mathbf{s}'. \quad (16)$$

Thus, Galerkin boundary-element methods reduce to the centroid collocation method when one uses one-point quadrature to approximate the integrals over β_j . In the simplest view, therefore, centroid collocation is a one-point approximation to the Galerkin method.

2.4. The Qualocation Discretization

The collocation and Galerkin approaches are not without their drawbacks. The Galerkin method requires a great deal of numerical integration and is therefore usually much slower; on the other hand, the relatively inexpensive centroid-collocation approach can be inaccurate when the residual varies quickly over the boundary elements. Tausch *et al.* noted this inaccuracy for the ICC formulation, and suggested an alternate approach called *qualocation* that retains the speed advantages of the collocation approach and the accuracy of Galerkin methods [48].

In qualocation, one reverses the order of the double integrals in Equation (12) to obtain

$$\int_{\beta_j} \int_{\beta_i} \mathbf{n}(\mathbf{s}) \cdot \frac{\mathbf{s}-\mathbf{s}'}{|\mathbf{s}-\mathbf{s}'|^3} ds ds' \quad (17)$$

so that the new outer integral can be approximated using one-point quadrature as

$$a_j \int_{\beta_i} \mathbf{n}(\mathbf{s}) \cdot \frac{\mathbf{s}-\mathbf{s}_j}{|\mathbf{s}-\mathbf{s}_j|^3} ds. \quad (18)$$

The new BEM matrix equation is $Bh = d$, where

$$d_i = -\frac{\Delta\epsilon(\mathbf{s}_i)}{4\pi\bar{\epsilon}(\mathbf{s}_i)} \int_{\beta_i} \left(\sum_k \frac{q_k}{\epsilon(\mathbf{r}_k)} \frac{\mathbf{s}'-\mathbf{r}_k}{|\mathbf{s}'-\mathbf{r}_k|^3} \cdot \mathbf{n}(\mathbf{s}') \right) ds' \quad (19)$$

and

$$B_{ij} = \alpha_i \delta_{ij} + \frac{\Delta\epsilon(\mathbf{s}_i)}{4\pi\bar{\epsilon}(\mathbf{s}_i)} a_j \int_{\beta_i} \left(\mathbf{n}(\mathbf{s}) \cdot \frac{\mathbf{s}-\mathbf{s}_j}{|\mathbf{s}-\mathbf{s}_j|^3} \right) ds. \quad (20)$$

3. TESTING THE COLLOCATION AND QUALOCATION METHODS

We simulate the analytically solvable problem of a single charge situated in a spherical dielectric [3, 60] (Figure 1). The sphere, which is centered at the origin, has radius 5 Å and dielectric constant ϵ_1 . A single discrete $+1e$ point charge is located inside the sphere at $x = 0$, $y = 0$, $z = 4\text{Å}$. The dielectric constant outside the sphere is $\epsilon_2 \ll \epsilon_1$. Although this situation seems reversed from the conditions described in Section 2.1, it serves as a prototype for an ion inside a confined space, such as inside the pore of a channel protein. For simplicity, we assume that the low-dielectric region extends to infinity [3].

We represent the spherical surface of the high dielectric body approximately using planar triangle boundary elements and take the dielectric constants to be $\epsilon_1 = 80$ and $\epsilon_2 = 2$. The analytical reaction potential [60] along the z axis is plotted in Figure 2(a). Also plotted are reaction potentials calculated numerically, using the collocation and qualocation discretizations of the ICC integral equation. As more boundary elements are used, both types of discretizations approach the analytical solution. For any given number of boundary elements, the qualocation discretization produces much more accurate electrostatic potentials than does the collocation approach. Similarly, for a desired accuracy, many more panels are required if one employs the collocation discretization instead of qualocation. For simulations reported in this paper, discretizations were generated using the widely used program MSMS [61], which can generate the solvent-excluded surface [62], although other definitions have been proposed recently (see, for example, Ref. 63).

In Figure 2(b) are plotted the errors (in kcal/mol/ e) between the computed reaction potentials and the analytical solution. Note that the vertical axes in Figure 2(b) are logarithmic, whereas those in Figure 2(a) are linear. The data in Figure 2(b) allow an approximate comparison to the recent MIBPB (Matched-Interface-and-Boundary for Poisson–Boltzmann) method introduced by Wei and collaborators [20, 64–66], a finite-difference method that employs a sophisticated approach to mitigate grid-based inaccuracies. Geng *et al.* have reported calculations for a single $+1e$ charge inside a low-dielectric sphere of radius 2 Å, embedded in a high dielectric medium. If the charge is situated 1 Å from the surface of

the sphere, the MIBPB method produces surface potentials accurate to approximately $1.5E-2$ kcal/mol/e. In the problem reported here (with a 5-\AA sphere and the ratios of the dielectric constants reversed), the collocation methods in the present problem are accurate to approximately $5E-2$ kcal/mol/e, and the qualocation methods are in error about $2E-3$ kcal/mol/e, or an order of magnitude better in accuracy. Note that the BEM error metrics are taken where the z axis intersects the sphere, whereas the reported MIBPB errors are the maximum error in surface potential over the whole dielectric boundary; however, the symmetry about the z axis suggests that the maximum error in the surface potential should be located where the axis intersects the sphere. These details suggest that the MIBPB and the BEM methods thus provide comparable accuracy for these discretizations. However, a much more detailed comparison of the MIBPB and qualocation BEM methods is outside the scope of the present work, and a subject of ongoing research.

3.1. Different Dielectric Ratios

It is well-known that the ICC integral equation becomes increasingly ill-conditioned as the ratio ϵ_1/ϵ_2 becomes large. In this limit, the interior dielectric becomes a conductor, and the problem represents a naïve second-kind formulation of the capacitance problem [56]. As the dielectric ratio goes to infinity, the integral equation is actually singular; that is, in this case no solution exists in general, and if a solution does exist, then there exist infinitely many solutions [31, 67]. The large ratio case ($\epsilon_1 > \epsilon_2 \gg 1$) describes many biological problems involving the movement of ions in solution. Most of biology occurs in salt solutions (physiological salines like Ringer or Tyrode solutions) that are good conductors, with resistivity approximately 50 Ohm-cm. On the other hand, lipid membranes are among the most perfect insulators known, with specific resistances commonly reaching 1 gigohm-cm². Proteins are (to first order) insulating objects, and almost all proteins have large hydrophobic regions that are very good insulators. The ill-conditioned case in the spherical test problem is thus an important case for biology and must be studied in some detail. The test problem of Boda *et al.* [3], which was designed to be in this domain, has $\epsilon_1/\epsilon_2 = 40$, and therefore the integral equation retains some of the ill-conditioning of the singular case.

The condition number κ of a matrix A , defined as the ratio of the largest singular value of A to its smallest singular value, is sometimes used to imply that a particular computational approach is accurate. Such an argument is at best incomplete, and at worst misleading. Although it is true that a large condition number implies an inaccurate simulation, it is not necessarily true that a small condition number implies an accurate simulation; in other words, reasonable conditioning is a necessary, but by no means sufficient, condition for a calculation to be accurate. To demonstrate this fact, in Figure 3 we plot the condition number of the qualocation and collocation BEM matrices as the ratio of dielectric constants varies from 10^{-3} to 10^3 . The condition number of the qualocation matrix grows rapidly as the ratio increases beyond one, which indicates that the qualocation BEM captures the ill-conditioning of the physical problem; that is, as the physical problem approaches the singular capacitance problem, the qualocation method is increasingly ill-conditioned. In contrast, the condition number of the collocation matrix does not change significantly. Clearly, the fact that the collocation matrix exhibits better conditioning does not imply that the collocation problem is easier to solve, or that collocation BEM is more accurate. For the present case, the lower condition number merely reflects the fact that the collocation discretization generates a low-accuracy representation of the badly conditioned problem.

We note that the dielectric ratio of interest in this test case is relevant for ion channels, ion-binding proteins, and enzymes that have pores or deep narrow clefts crucial to their biological function. Other proteins are different and have an enclosed volume that is the protein (with low dielectric constant) where the exterior region is the higher dielectric solvent [9, 10, 68].

3.2. Higher-Order Approximations to the Galerkin Method

We now compare the speed of the collocation and qualocation methods, and present a fast approximation to the qualocation method. As discussed in Section 2, the collocation and qualocation methods can both be interpreted as one-point approximations to a Galerkin BEM [48]. Higher-order collocation-like and the qualocation-like approximations can also be employed [51], and in the limit of infinitely-high-order approximations the methods generate identical solutions. It is instructive to see the effects on accuracy of using different approximations. To illustrate these effects, we have used the same test geometry as before (see Figure 1), and solved BEM problems using 3-point, 10-point, and 18-point approximations to the integrals that are approximated with midpoint quadrature in the collocation and qualocation methods (Equations (15) and (20)). Figure 4 contains plots of the reaction potentials calculated using these methods. In the Figure, the results from using successively higher-order quadrature rules are plotted using progressively larger symbols. All of the approximations that use qualocation-like discretizations generate nearly identical potentials, which indicates that the one-point approximation employed in qualocation is already very accurate. Consequently, the qualocation results in Figure 4 are almost indistinguishable. However, as can be seen in the Figure, the collocation-like methods generate quite different potentials. Unfortunately, although it is possible to assess theoretically the accuracy of a particular integral as the order of the numerical integration scheme is increased, it is not straightforward to analyze the accuracy of computed solvation free energies in a similarly rigorous manner.

It must be emphasized that in the present work, the BEM matrices are formed explicitly and therefore the time required to compute the BEM matrices is directly proportional to the number of points used in the integral approximation. Also, for the planar triangles we have used to approximate the surface, the boundary-element integrals in Equations (15) and (20) can be computed analytically and require nearly identical computational work [69, 70]. As a result, essentially the same amount of time is required to compute the basic (1-point) collocation and qualocation matrices. The 3-point collocation-like method requires three times the amount of work to compute the 1-point collocation matrix, and the 10-point qualocation-like method requires ten times the amount of work required for the 1-point qualocation matrix. We note that if instead of forming the BEM matrix explicitly, one employs a fast algorithm such as the fast-multipole method (FMM) [46, 71] or the FFTSVD [22, 72] method, the higher-order quadrature approaches will not give rise to such a precise correspondence with computational cost.

3.3. Interactions between Multiple Charges

Proteins contain many permanent (i.e., fixed) charges, usually on acid and basic side chains. Ionic solutions contain a multitude of permanent charges, on the order of 10^{23} per liter (dm^3). We therefore examine how the method of BEM discretization changes calculations of the interactions between multiple charges. We have studied two systems using the geometry of Figure 1 with additional charges. In the first test case, two charges are present in the solvent (that is, inside the high-dielectric sphere). One $+1e$ charge is located at $(0, 0, 4)$ as before and the other charge, also $+1e$, is located at $(-4, 0, 0)$. Figure 5 contains plots of the reaction potentials along the z axis, calculated using the collocation and qualocation discretizations. In the second test case, a $+1e$ charge at $(0, 0, 4)$ is balanced across the sphere boundary by a $-1e$ charge inside the protein at $(0, 0, 6)$. Figure 6 contains plots of the reaction potentials for this test geometry. It is clear that in both test cases the qualocation method offers much better accuracy than collocation. In both Figure 5 and Figure 6, higher-resolution calculations (those with larger numbers of boundary elements, as denoted in the legend by N) are denoted by larger symbols. The improved accuracy of the qualocation method results in the qualocation curves lying nearly on top of one another. Note, however,

that in Figure 6 the lowest-resolution calculation differs significantly even for the qualocation method in the proximity of the charge in the high-dielectric region.

3.4. Accelerated Qualocation

We now address the efficiency of simulations of ionic solutions—that is, of problems with many charges in the solvent. It can be seen from Equations (13) and (14), which are the expressions for the right-hand-side (RHS) vectors associated with the qualocation and collocation methods, that the qualocation method requires more computational work to form the RHS, than the collocation method. The collocation method requires only the calculation of the potential at the centroid of each boundary element; the qualocation method requires integration of the potential over each boundary element. We therefore turn to situations in which calculation of the RHS takes significant time.

An example of such a scenario can be found in the use of Monte-Carlo (MC) and some molecular-dynamics (MD) methods to study the electrostatic interactions between biomolecules and ionic solutions [3, 26, 73–85]. In such calculations, the protein is usually treated as a rigid dielectric body and ions are treated as point charges in the high-dielectric solvent. Each MC step entails moving an ion to a random location, and accepting or rejecting the move depending on the resulting change in energy; at each step one must solve the electrostatic problem. Typically, hundreds of millions or billions of steps are used [83]. In these MC simulations, the right-hand side of the BEM problem is different at each step while the BEM matrix remains the same. As a result, even when the matrix is decomposed once via LU factorization (at a cost that grows cubically with the number of unknowns), the time associated with calculating all of the right-hand sides can represent a substantial portion of the total. This situation contrasts with most BEM simulations, in which calculation of the matrix entries, compression of the BEM matrix [46], or LU factorization represent the dominant computational cost, and the time required for calculating the right-hand side is insignificant.

The boundary-element integrals required for forming the qualocation RHS can be accurately approximated for the same computational cost required for the collocation RHS, if it is known *a priori* that charges will not be too close to the boundary elements. To demonstrate this, we simulated the test geometry with a single point charge, using analytical integration methods to evaluate the integrals associated with the qualocation RHS, and also using one-point quadrature. Figure 7 is a plot of the calculated reaction potentials using the two methods for forming the RHS; thus, the plot associated with the qualocation method is the same as in Figure 2. The one-point RHS method incurs approximately 1% error relative to the analytical integration method; in general, however, the accuracy depends on the details of the problem.

The improved accuracy of the qualocation method can allow a reduction in the number of boundary elements used for simulation, once one prescribes the desired level of accuracy. To estimate the magnitude of the time savings, we computed the time required to solve matrix problems with dimensions equal to the BEM problems studied here and in Boda *et al.* [3]. Using MATLAB [86] we solved 1000 linear systems for each problem and measured the time required to repeatedly apply the dense L and U factors to solve the systems. For dense nonsingular systems, the solve time is essentially independent of the entries of the L and U factors themselves. The qualocation simulation of a 356-variable problem was accurate to within approximately two percent, and 1000 linear solves required 0.939 seconds. The 1470-variable qualocation problem required 17.995 seconds and was accurate to about one percent. For problems of dimensions employed by Boda *et al.*, the time required for the 512-variable problem (two-percent accuracy) was 2.004 seconds, and 36.821 seconds were required for the 2048-variable problem, reaching one-percent accuracy.

Thus, for this level of accuracy and simulating problems of these dimensions, the qualocation method is approximately twice as fast for repeated matrix solves using the L and U factors. This improvement is not expected for all levels of accuracy, however. Qualocation's performance advantage appears to grow as higher accuracy is demanded [50].

4. DISCUSSION

We have presented the collocation and qualocation approaches to solving the ICC boundary-integral equation for electrostatic analysis of channel proteins. Our results illustrate that computation of the electric field, which is of central importance in the ICC equation, needs to be performed carefully. Though both collocation and qualocation use a simple form of numerical integration, midpoint quadrature, the qualocation method provides significantly better accuracy. As demonstrated by Tausch *et al.*, the improvement can be attributed to the simple fact that the electric potential due to a dipole distribution varies more slowly than does the normal electric field due to a monopole distribution [48]. This improvement in accuracy allows a reduction in computation time because the dielectric boundaries can be discretized using fewer boundary elements. Our calculations have employed a simple model geometry that possesses an analytical solution while retaining important characteristics of interactions between ions and channel proteins; other recent work has compared qualocation and collocation methods for simulating atomistically detailed proteins [87].

Our results suggest that the accuracy advantage of the qualocation method is most important when permanent charges lie in the region of high dielectric, e.g., when ions like Na⁺, K⁺, Ca⁺⁺ or Cl⁻ are inside channels or near active sites of proteins, balancing the fixed (i.e., permanent) charge of the side chains of the protein. This result is in keeping with the analysis of Greengard and Lee [49]. Protein enzymes and channels are characterized experimentally by measurements with a variety of ions and concentrations. Simulations designed to reproduce these types of experiments will therefore benefit particularly from the qualocation method.

The qualocation and collocation methods we have presented take advantage of special properties of planar boundary elements with straight edges. Analytical methods can be used to rapidly evaluate the resulting integrals [69, 70] while accounting for singularities exactly. Clearly, flat boundary elements describe the curved surfaces of ions and proteins less well than curved boundary elements [3, 45, 88]. For computations in which memory is a limiting factor, curved elements do offer improved accuracy [88]. However, the integrals associated with curved boundary elements usually require much more time than the integrals associated with flat elements [88], and require considerably more complex implementation [89]. These competing influences on simulation time and accuracy make it difficult to predict *a priori* whether a planar- or curved-element approach will be preferable for a given simulation.

The generation of appropriate surface discretizations, whether using planar or curved elements, is another factor that complicates the analysis of the merits of these two simulation approaches. It can be difficult to find curved-element discretizations of the complex surfaces often used to model molecules and proteins in solution [12, 45, 88, 90, 91], even if the boundary can be described analytically [62, 92, 93]. In contrast, there exist numerous algorithms for calculating planar-element representations of these surfaces (see, for instance, [61, 92, 94]), and efficient and robust implementations are widely available [95, 96].

However, a case may certainly be made for curved-element BEM when a dielectric boundary remains unchanged throughout a Monte Carlo simulation, as in several recent investigations [3, 24, 26, 73]), and the boundary can be easily described by a few thousand curved elements (such that dense-matrix memory limitations are not an issue). Under these circumstances, the overall MC calculation is not necessarily dominated by the $O(n^3)$ cost to

form the LU factors (a computation that is performed only once), but rather by the $O(n^2)$ cost of applying the factors at each MC step. Efficient methods for MC simulations with larger memory requirements are a subject of ongoing work. Preconditioned Krylov-subspace iterative methods such as GMRES [97], used in combination with algorithms that rapidly approximate matrix–vector multiplication, such as the fast-multipole method [46, 47] represent a promising approach [21, 22, 71, 98–101].

Acknowledgments

The submitted manuscript has been created by the University of Chicago, LLC as Operator of Argonne National Laboratory (“Argonne”). Argonne, a U.S. Department of Energy Office of Science laboratory, is operated under Contract No. DE-AC02-06CH11357. The U.S. Government retains for itself, and others acting on its behalf, a paid-up, nonexclusive, irrevocable worldwide license in said article to reproduce, prepare derivative works, distribute copies to the public, and perform publicly and display publicly, by or on behalf of the Government.

The authors would like to express gratitude to M. Anitescu for useful discussions, to D. Boda for sharing analytical results for the sphere example, to K. Nabors and J. K. White for making available boundary-element integration software. J. P. B. acknowledges funding from a Wilkinson Fellowship in Scientific Computing funded by the Mathematical, Information, and Computational Sciences Division Subprogram of the Office of Advanced Scientific Computing Research, Office of Science, U. S. Dept. of Energy, under Contract DE-AC02-06CH11357. R. S. E. acknowledges support from the National Institutes of Health, grant GM076013.

References

1. Clapham DE. Calcium signaling. *Cell*. 2007; 131:1047–1058. [PubMed: 18083096]
2. Graf P, Kurnikova MG, Coalson RD, Nitzan A. Comparison of dynamic lattice Monte Carlo simulations and the dielectric self-energy Poisson–Nernst–Planck continuum theory for model ion channels. *Journal of Physical Chemistry B*. 2004; 108:2006–2015.
3. Boda D, Voliskó M, Eisenberg B, Nonner W, Henderson D, Gillespie D. The effect of protein dielectric coefficient on the ionic selectivity of a calcium channel. *Journal of Chemical Physics*. 2006; 125(034901)
4. Ba tu T, Kuyucak S. Role of the dielectric constants of membrane proteins and channel water in ion permeation. *Biophysical Journal*. 2003; 84:2871–2882. [PubMed: 12719220]
5. Barthel, JMG.; Krienke, H.; Kunz, W. *Physical Chemistry of Electrolyte Solutions: Modern Aspects*. 1. Steinkopff-Verlag; 2002.
6. Svensson B, Jonsson B, Woodward CE, Linse S. Ion-binding properties of calbindin-D9K – a Monte-Carlo simulation study. *Biochemistry*. 1991; 30(21):5209–5217. [PubMed: 2036387]
7. Nonner W, Catacuzzeno L, Eisenberg B. Binding and selectivity in L-type calcium channels: a mean spherical approximation. *Biophysical Journal*. 2000; 79:1976–1992. [PubMed: 11023902]
8. Dahirel V, Jardat M, Dufrêche J-F, Turq P. Toward the description of electrostatic interactions between globular proteins: Potential of mean force in the primitive model. *Journal of Chemical Physics*. 2007; 127(095101)
9. Warwicker J, Watson HC. Calculation of the electric potential in the active site cleft due to alpha-helix dipoles. *Journal of Molecular Biology*. 1982; 157:671–679. [PubMed: 6288964]
10. Sharp KA, Honig B. Electrostatic interactions in macromolecules: Theory and applications. *Annual Review of Biophysics and Biophysical Chemistry*. 1990; 19:301–332.
11. Sharp KA, Honig B. Calculating total electrostatic energies with the nonlinear Poisson–Boltzmann equation. *Journal of Physical Chemistry*. 1990; 94(19):7684–7692.
12. Juffer AH, Botta EFF, van Keulen BAM, van der Ploeg A, Berendsen HJC. The electric potential of a macromolecule in a solvent: A fundamental approach. *Journal of Computational Physics*. 1991; 97(1):144–171.
13. Honig B, Sharp K, Yang AS. Macroscopic models of aqueous solutions: Biological and chemical applications. *Journal of Physical Chemistry*. 1993; 97(6):1101–1109.
14. Holst, MJ. PhD thesis. Univ. of Ill; Urbana-Champaign: 1993. Multilevel Methods for the Poisson-Boltzmann Equation.

15. Zhou HX. Macromolecular electrostatic energy within the nonlinear Poisson–Boltzmann equation. *J Chem Phys.* 1994; 100:3152–3162.
16. Baker NA, Sept D, Holst MJ, McCammon JA. Electrostatics of nanoystems: Application to microtubules and the ribosome. *Proceedings of the National Academy of Sciences of the USA.* 2001; 98:10037–10041. [PubMed: 11517324]
17. Rocchia W, Alexov E, Honig B. Extending the applicability of the nonlinear Poisson–Boltzmann equation: Multiple dielectric constants and multivalent ions. *Journal of Physical Chemistry B.* 2001; 105:6507–6514.
18. Baker NA. Biomolecular applications of Poisson–Boltzmann methods. *Rev Comp Chem.* 2005; 21:349–379.
19. Bertonati C, Honig B, Alexov E. Poisson–Boltzmann calculations of nonspecific salt effects on protein–protein binding free energies. *Biophysical Journal.* 2007; 92:1891–1899. [PubMed: 17208980]
20. Yu SN, Zhou YC, Wei GW. Matched interface and boundary (MIB) method for elliptic problems with sharp-edged interfaces. *Journal of Computational Physics.* 2007; 224(2):729–756.
21. Lu B, Zhou YC, Holst MJ, McCammon JA. Recent progress in numerical methods for the Poisson–Boltzmann equation in biophysical applications. *Communications in Computational Physics.* 2008; 3(5):973–1009.
22. Altman, MDo; Bardhan, JP.; White, JK.; Tidor, B. Accurate solution of multi-region continuum electrostatic problems using the linearized Poisson–Boltzmann equation and curved boundary elements. *Journal of Computational Chemistry.* 2009; 30:132–153. [PubMed: 18567005]
23. Simonov NA, Mascagni M, Fenley MO. Monte Carlo-based linear Poisson–Boltzmann approach makes accurate salt-dependent solvation free energy predictions possible. *Journal of Chemical Physics.* 2007; 127:185105. [PubMed: 18020668]
24. de Carvalho SJ, Fenley MO, da Silva FLB. Protein–ion binding process on finite macromolecular concentration. a poisson–boltzmann and monte carlo study. *Journal of Physical Chemistry B.* 2008
25. Prabhu NV, Panda M, Yang Q, Sharp KA. Explicit ion, implicit water solvation for molecular dynamics of nucleic acids and highly charged molecules. *Journal of Computational Chemistry.* 2008; 29:1113–1130. [PubMed: 18074338]
26. Boda D, Valiskó M, Henderson D, Gillespie D, Eisenberg B, Gilson MK. Ions and inhibitors in the binding site of HIV protease: Comparison of Monte Carlo simulations and the linearized Poisson–Boltzmann theory. *Biophysical Journal.* 2009; 96:1293–1306. [PubMed: 19217848]
27. Tanford C, Kirkwood JG. Theory of protein titration curves I. General equations for impenetrable spheres. *Journal of the American Chemical Society.* 1957; 59:5333–5339.
28. Gilson MK, Rashin A, Fine R, Honig B. On the calculation of electrostatic interactions in proteins. *Journal of Molecular Biology.* 1985; 183:503–516. [PubMed: 3874968]
29. Klapper I, Hagstrom R, Fine R, Sharp K, Honig B. Focusing of electric fields in the active site of Cu-Zn superoxide dismutase: Effects of ionic strength and amino-acid modification. *Proteins: Structure, Function, Genetics.* 1986; 1:47–59.
30. Holst M, Saied F. Multigrid solution of the Poisson–Boltzmann equation. *Journal of Computational Chemistry.* 1993; 14:105–113.
31. Atkinson, KE. *The Numerical Solution of Integral Equations of the Second Kind.* Cambridge University Press; 1997.
32. Shaw PB. Theory of the Poisson Green’s-function for discontinuous dielectric media with an application to protein biophysics. *Physical Review A.* 1985; 32(4):2476–2487. [PubMed: 9896362]
33. Levitt DG. Electrostatic calculations for an ion channel. I. Energy and potential profiles and interactions between ions. *Biophysical Journal.* 1978; 22:209–219. [PubMed: 656542]
34. Jordan PC. Electrostatic modeling of ion pores: I. Energy barriers and electric field profiles. *Biophysical Journal.* 1982; 39:157–164. [PubMed: 6288132]
35. Jordan PC. Electrostatic modeling of ion pores: II. Effects attributable to the membrane dipole potential. *Biophysical Journal.* 1983; 41:189–195. [PubMed: 6188503]
36. Hoyles M, Kuyucak S, Chung SH. Energy barrier presented to ions by the vestibule of the biological membrane channel. *Biophysical Journal.* 1996; 70:1628–1642. [PubMed: 8785322]

37. Hoyles M, Kuyucak S, Chung SH. Solutions of Poisson's equation in channel-like geometries. *Computer Physics Communications*. 1998; 115:45–68.
38. Miertus S, Scrocco E, Tomasi J. Electrostatic interactions of a solute with a continuum – a direct utilization of *ab initio* molecular potentials for the prevision of solvent effects. *Chemical Physics*. 1981; 55(1):117–129.
39. Tomasi J, Mennucci B, Cammi R. Quantum mechanical continuum solvation models. *Chemical Reviews*. 2005; 105:2999–3093. [PubMed: 16092826]
40. Chipman DN. Comparison of solvent reaction field representations. *Theoretical Chemistry Accounts*. 2002; 107(2):80–89.
41. Zauhar RJ, Morgan RS. A new method for computing the macromolecular electric-potential. *Journal of Molecular Biology*. 1985; 186(4):815–820. [PubMed: 4093987]
42. Zauhar RJ, Morgan RS. The rigorous computation of the molecular electric potential. *Journal of Computational Chemistry*. 1988; 9(2):171–187.
43. Zauhar RJ, Morgan RS. Computing the electric-potential of biomolecules: application of a new method of molecular-surface triangulation. *Journal of Computational Chemistry*. 1990; 11(5):603–622.
44. Zauhar RJ, Varnek A. A fast and space-efficient boundary element method for computing electrostatic and hydration effects in large molecules. *Journal of Computational Chemistry*. 1996; 17:864–877.
45. Liang J, Subramaniam S. Computation of molecular electrostatics with boundary element methods. *Biophysical Journal*. 1997; 73(4):1830–1841. [PubMed: 9336178]
46. Greengard L, Rokhlin V. A fast algorithm for particle simulations. *Journal of Computational Physics*. 1987; 73:325–348.
47. Greengard, L. *The Rapid Evaluation of Potential Fields in Particle Systems*. MIT Press; 1988.
48. Tausch J, Wang J, White J. Improved integral formulations for fast 3-D method-of-moment solvers. *IEEE Transactions on Computer-Aided Design of Integrated Circuits and Systems*. 2001; 20(12):1398–1405.
49. Greengard L, Lee JY. Electrostatics and heat conduction in high contrast composite materials. *Journal of Computational Physics*. 2006; 211:64–76.
50. Altman, MD.; Bardhan, JP.; White, JK.; Tidor, B. An efficient and accurate surface formulation for biomolecule electrostatics in non-ionic solution. *Engineering in Medicine and Biology Conference (EMBC)*; 2005.
51. Bardhan, JP. Numerical solution of boundary integral equations for molecular electrostatics. MCS Division, Argonne National Laboratory; 2008. Preprint ANL/MCS-P1527-0708
52. Hille, B. *Ionic Channels of Excitable Membranes*. 3. Sinauer Associates Inc; 2001.
53. Ashcroft, FM. *Ion channels and disease: Channelopathies*. 1. Academic Press; 2000.
54. Rao SM, Sarkar TK, Harrington RF. The electrostatic field of conducting bodies in multiple dielectric media. *IEEE Transactions on Microwave Theory and Techniques*. 1984; 32(11):1441–1448.
55. Purisima EO. Fast summation boundary element method for calculating solvation free energies of macromolecules. *Journal of Computational Chemistry*. 1998; 19(13):1494–1504.
56. Jaswon, MA.; Symm, GT. *Integral equation methods in potential theory and elastostatics*. Academic Press; London: 1977.
57. Kress, R. *Linear Integral Equations*. Springer-Verlag; Berlin: 1989.
58. Hsiao GC, Wendland WL. Boundary element methods: foundations and error analysis. *Encyclopedia of Computational Mechanics*. 2004
59. Ruehli AE, Brennan PA. Efficient capacitance calculations for three-dimensional multiconductor systems. *IEEE Transactions on Microwave Theory and Techniques*. 1973; 21:76–82.
60. Griffiths, DJ. *Introduction to Electrodynamics*. 3. Benjamin Cummings; 1999.
61. Sanner M, Olson AJ, Spehner JC. Reduced surface: An efficient way to compute molecular surfaces. *Biopolymers*. 1996; 38:305–320. [PubMed: 8906967]
62. Richards FM. Areas, volumes, packing, and protein structure. *Annual Review of Biophysics and Bioengineering*. 1977; 6:151–176.

63. Bates PW, Wei GW, Zhao S. Minimal molecular surfaces and their applications. *Journal of Computational Chemistry*. 2008; 29:380–391. [PubMed: 17591718]
64. Yu SN, Geng WH, Wei GW. Treatment of geometric singularities in implicit solvent models. *Journal of Chemical Physics*. 2007; 126(24):244108. [PubMed: 17614538]
65. Geng WH, Yu SN, Wei GW. Treatment of charge singularities in implicit solvent models. *Journal of Chemical Physics*. 2007; 127:114106. [PubMed: 17887827]
66. Zhou YC, Feig M, Wei GW. Highly accurate biomolecular electrostatics in continuum dielectric environments. *Journal of Computational Chemistry*. 2008; 29:87–97. [PubMed: 17508411]
67. Tausch J, White JK. Second-kind integral formulations of the capacitance problem. *Advances in Computational Mathematics*. 1998; 9:217–232.
68. Honig B, Nicholls A. Classical electrostatics in biology and chemistry. *Science*. 1995; 268:1144–1149. [PubMed: 7761829]
69. Hess JL, Smith AMO. Calculation of non-lifting potential flow about arbitrary three-dimensional bodies. *Journal of Ship Research*. 1962; 8(2):22–44.
70. Newman JN. Distribution of sources and normal dipoles over a quadrilateral panel. *Journal of Engineering Mathematics*. 1986; 20(2):113–126.
71. Lu BZ, Cheng XL, Huang J, McCammon JA. Order N algorithm for computation of electrostatic interactions in biomolecular systems. *Proceedings of the National Academy of Sciences of the USA*. 2006; 103(51):19314–19319. [PubMed: 17148613]
72. Altman MD, Bardhan JP, Tidor B, White JK. FFTSV: A fast multiscale boundary-element method solver suitable for BioMEMS and biomolecule simulation. *IEEE Transactions on Computer-Aided Design of Integrated Circuits and Systems*. 2006; 25:274–284.
73. Xin W, Juffer AH. A boundary element formulation of protein electrostatics with explicit ions. *Journal of Computational Physics*. 2007; 223:416–435.
74. Chung SH, Allen T, Hoyles M, Kuyucak S. Permeation of ions across the potassium channel: Brownian dynamics studies. *Biophysical Journal*. 1999; 77:2517–2533. [PubMed: 10545353]
75. Kurnikova MG, Coalson RD, Graf P, Nitzan A. A lattice relaxation algorithm for three-dimensional Poisson–Nernst–Planck theory with application to ion transport through the gramicidin A channel. *Biophysical Journal*. 1999; 76:642–656. [PubMed: 9929470]
76. Graf P, Nitzan A, Kurnikova MG, Coalson RD. A dynamic lattice Monte Carlo model of ion transport in inhomogeneous dielectric environments: method and implementation. *Journal of Physical Chemistry B*. 2000; 104:12324–12338.
77. Im W, Seefeld S, Roux B. A grand canonical Monte Carlo–Brownian dynamics algorithm for simulating ion channels. *Biophysical Journal*. 2000; 79:788–801. [PubMed: 10920012]
78. Im W, Roux B. Brownian dynamics simulations of ions channels: a general treatment of electrostatic reaction fields for molecular pores of arbitrary geometry. *Journal of Chemical Physics*. 2001; 115:4850–4861.
79. Boda D, Busath D, Eisenberg B, Henderson D, Nonner W. Monte Carlo simulations of ion selectivity in a biological Na^+ channel: charge-space competition. *Physical Chemistry Chemical Physics*. 2002; 4:5154–5160.
80. Mamonov AB, Coalson RD, Nitzan A, Kurnikova MG. The role of the dielectric barrier in narrow biological channels: a novel composite approach to modeling single-channel currents. *Biophysical Journal*. 2003; 84:3646–3661. [PubMed: 12770873]
81. Im W, Roux B. Ion permeation and selectivity of OmpF porin: a theoretical study based on molecular dynamics, Brownian dynamics, and continuum electrodiffusion theory. *Journal of Molecular Biology*. 2002; 322:851–869. [PubMed: 12270719]
82. Boda D, Varga T, Henderson D, Busath D, Nonner W, Gillespie D, Eisenberg B. Monte Carlo simulation study of a system with a dielectric boundary: application to calcium channel selectivity. *Molecular Simulation*. 2004:89–96.
83. Boda D, Nonner W, Valiskó M, Henderson D, Eisenberg B, Gillespie D. Steric selectivity in Na^+ channels arising from protein polarization and mobile side chains. *Biophysical Journal*. 2007; 93:1960–1980. [PubMed: 17526571]
84. Boda D, Nonner W, Henderson D, Eisenberg B, Gillespie D. Volume exclusion in calcium selective channels. *Biophysical Journal*. 2008; 94:3486–3496. [PubMed: 18199663]

85. Vora T, Bisset D, Chung SH. Conduction of Na^+ and K^+ through the NaK channel: Molecular and Brownian dynamics studies. *Biophysical Journal*. 2008; 95:1600–1611. [PubMed: 18456826]
86. *Matlab v.6*. Mathworks, Inc.
87. Bardhan JP. Numerical solution of boundary-integral equations for molecular electrostatics. *Journal of Chemical Physics*. 2009; 130:094102. [PubMed: 19275391]
88. Bardhan JP, Altman MD, White JK, Tidor B. Numerical integration techniques for curved-panel discretizations of molecule–solvent interfaces. *Journal of Chemical Physics*. 2007; 127:014701. [PubMed: 17627358]
89. Guermond JL. Numerical quadratures for layer potentials over curved domains in \mathbb{R}^3 . *SIAM Journal on Numerical Analysis*. 1992; 29(5):1347–1369.
90. Bajaj CL, Pascucci V, Shamir A, Holt RJ, Netravali AN. Dynamic maintenance and visualization of molecular surfaces. *Discrete Applied Mathematics*. 2003; 127(1):23–51.
91. Zauhar RJ. SMART: A solvent-accessible triangulated surface generator for molecular graphics and boundary-element applications. *Journal of Computer-Aided Molecular Design*. 1995; 9(2): 149–159. [PubMed: 7608746]
92. Connolly ML. Analytical molecular surface calculation. *Journal of Applied Crystallography*. 1983; 16:548–558.
93. Vorobjev YN, Hermans J. SIMS: computation of a smooth invariant molecular surface. *Biophysical Journal*. 1997; 73:722–732. [PubMed: 9251789]
94. Totrov M, Abagyan R. The contour-buildup algorithm to calculate the analytical molecular surface. *Journal of Structural Biology*. 1996; 116(1):138–143. [PubMed: 8742735]
95. Connolly, M. Molecular surface package. 2000. <http://connolly.best.vwh.net>
96. Sanner, MF. Molecular surface computation home page. 1996. <http://www.scripps.edu/sanner/html/msmshome.html>
97. Saad Y, Schultz M. GMRES: A generalized minimal residual algorithm for solving nonsymmetric linear systems. *SIAM Journal of Scientific and Statistical Computing*. 1986; 7:856–869.
98. Bharadwaj R, Windemuth A, Sridharan S, Honig B, Nicholls A. The fast multi-pole boundary element method for molecular electrostatics: An optimal approach for large systems. *Journal of Computational Chemistry*. 1995; 16(7):898–913.
99. Fenley MO, Olson WK, Chua K, Boschitsch AH. Fast adaptive multipole method for computation of electrostatic energy in simulations of polyelectrolyte DNA. *Journal of Computational Chemistry*. 1996; 17(8):976–991.
100. Vorobjev YN, Scheraga HA. A fast adaptive multigrid boundary element method for macromolecular electrostatic computations in a solvent. *Journal of Computational Chemistry*. 1997; 18(4):569–583.
101. Boschitsch AH, Fenley MO, Zhou HX. Fast boundary element method for the linear Poisson–Boltzmann equation. *Journal of Physical Chemistry B*. 2002; 106(10):2741–54.

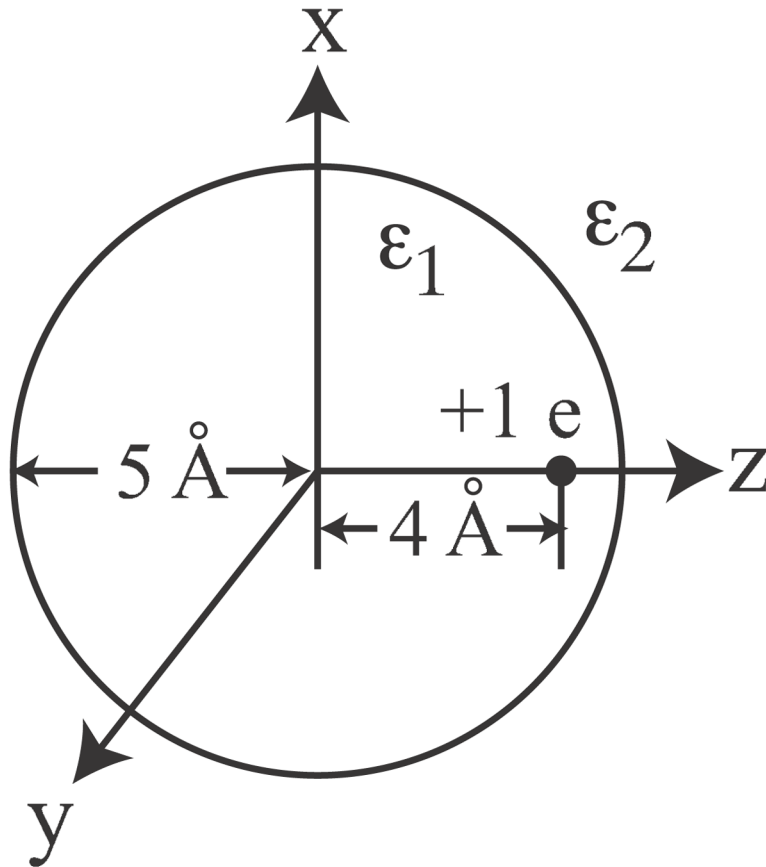


Figure 1. The geometry of the model problem. A dielectric sphere of radius 5 \AA , centered at the origin, with dielectric constant ϵ_1 is embedded in a homogeneous dielectric medium of dielectric constant ϵ_2 . A single discrete point charge of value $+1 e$ is located at $(0, 0, 4 \text{ \AA})$.

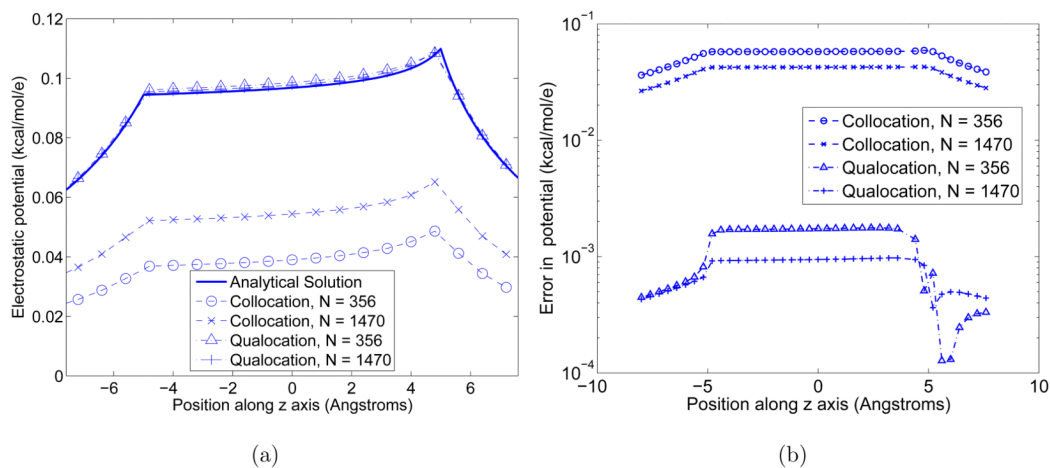


Figure 2.

Reaction potentials, and errors relative to an analytical solution, calculated along the z axis using the centroid-collocation and qualocation discretizations, for a sphere of radius 5 \AA and dielectric constant 80 embedded in an infinite medium of dielectric constant 2, with a single $+1e$ charge located at $(0, 0, 4 \text{ \AA})$. (a) Computed and analytical reaction potentials. Electrostatic potentials are in kcal/mol/e. (b) Error between computed reaction potentials and analytical solution, in kcal/mol/e.

Electrostatic potentials are in kcal/mol/e. (b) Error between computed reaction potentials and analytical solution, in kcal/mol/e.

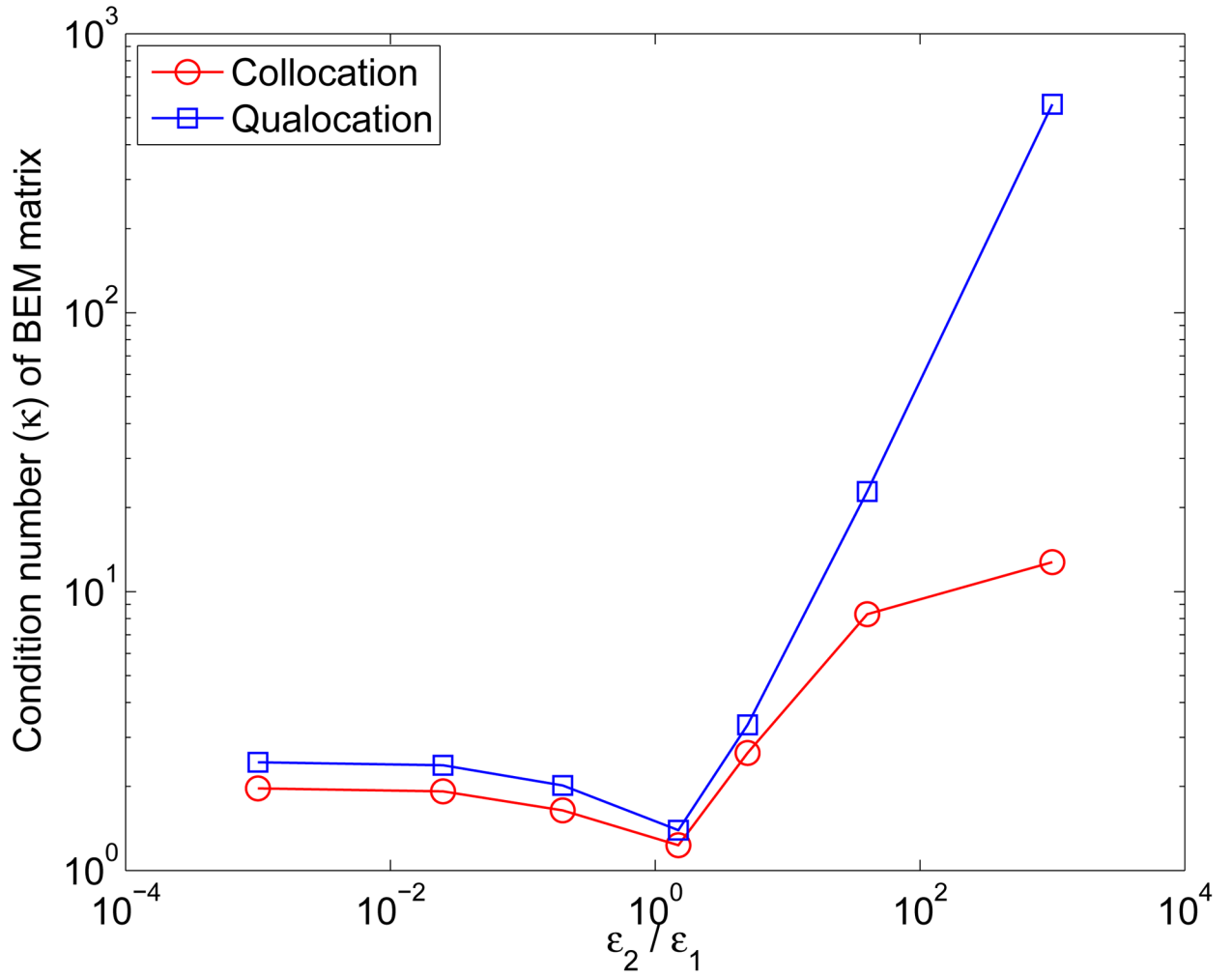


Figure 3.

Condition numbers of the qualocation and centroid-collocation matrices, for the same problem geometry as in Figure 2 with the 356-element surface discretization, as the dielectric ratio ϵ_2/ϵ_1 varies. The dielectric constants were 1/1000, 2/80, 4/20, 6/4, 20/4, 80/2 (the same constants used by Boda *et al.* [3]), and 1000/1.

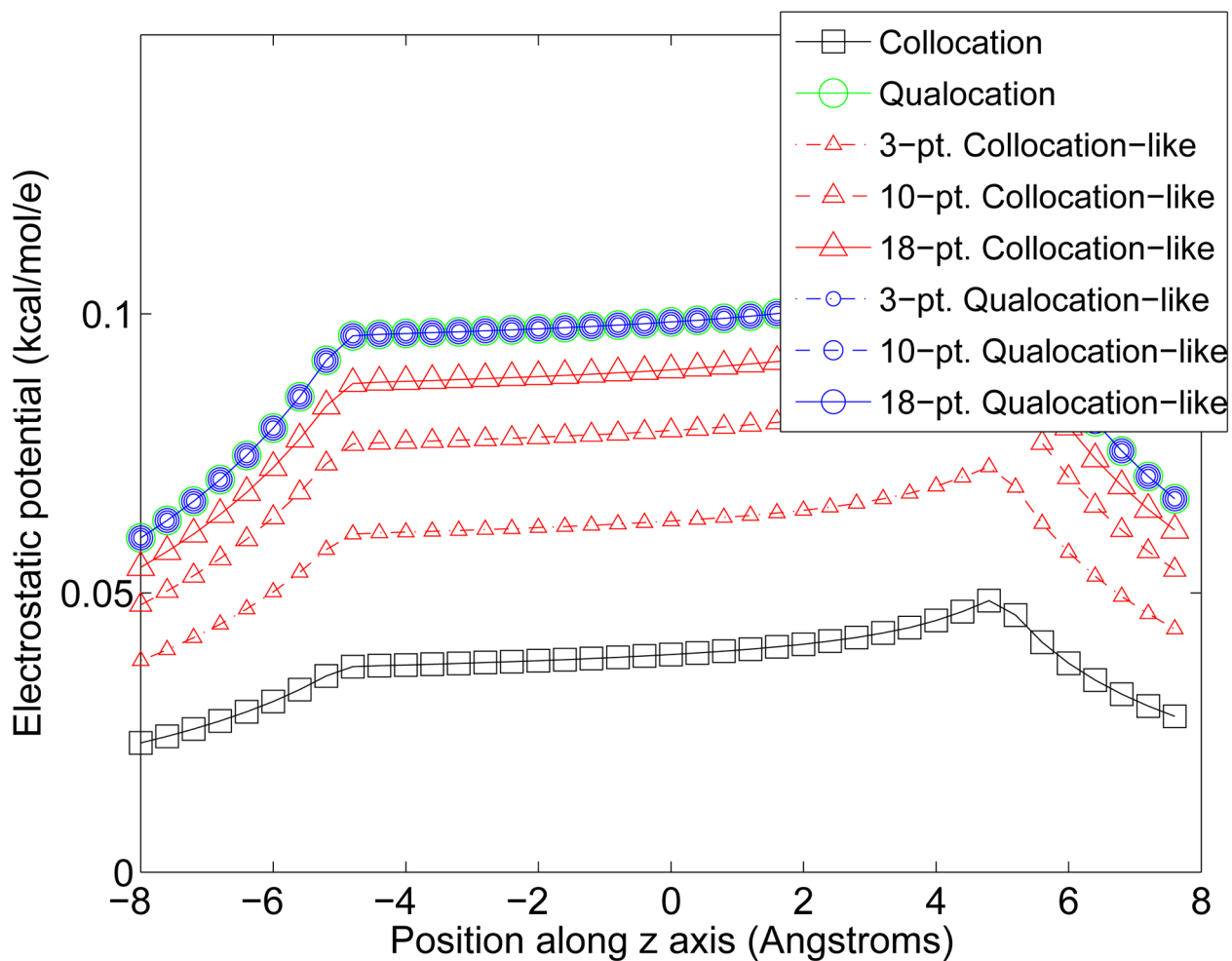


Figure 4.

Accuracy of calculated reaction potentials when higher-order quadrature methods are employed to approximate the Galerkin integrals, using qualocation-like and collocation-like discretizations. The problem geometry is the same as used in Figure 2. The qualocation results, denoted by solid lines with circles of varying sizes, are nearly indistinguishable.

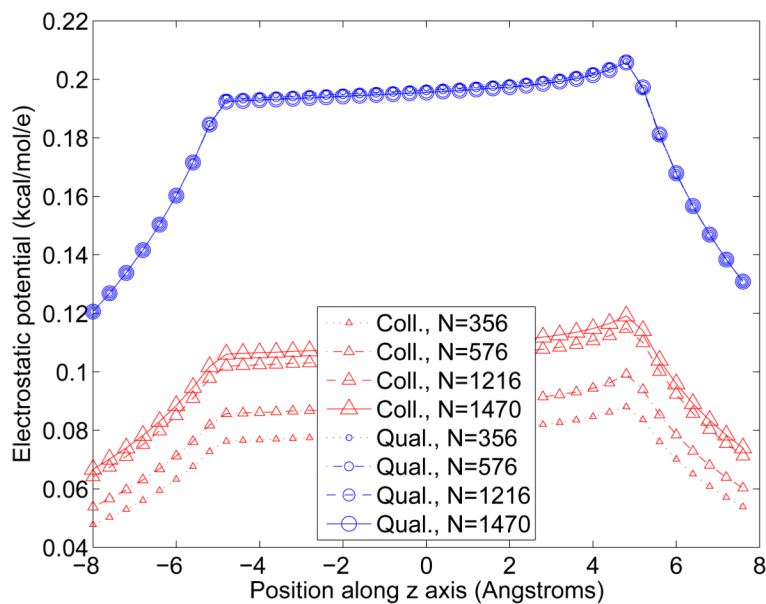


Figure 5.

Accuracy of centroid-collocation and qualocation methods for problems with multiple charges in the high-dielectric region. The problem geometry is the same as used in Figure 2, with an extra $+1e$ charge placed at $(-4 \text{ \AA}, 0, 0)$. The qualocation results, denoted by solid lines with circles of varying sizes, are nearly indistinguishable.

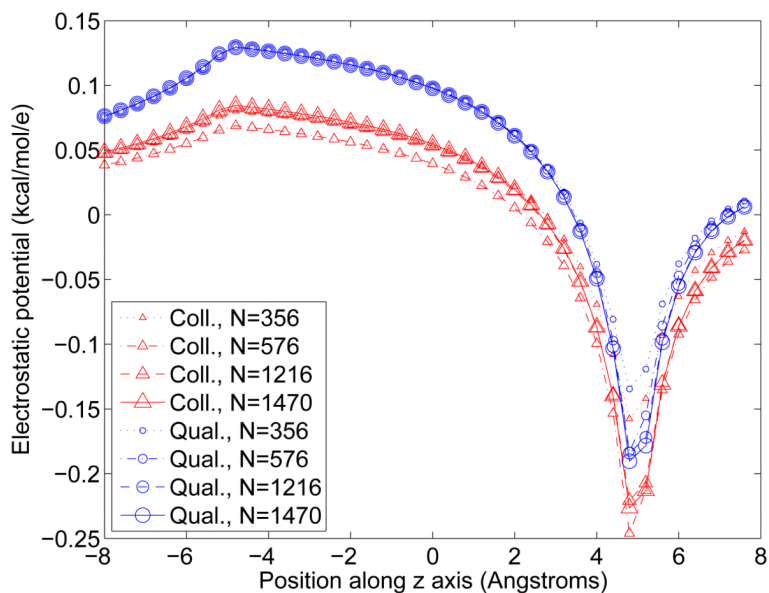


Figure 6.

Accuracy of centroid-collocation and qualocation methods for problems with charges in both the high- and low-dielectric regions. The problem geometry is the same as used in Figure 2, with an additional $-1e$ charge placed in the low-dielectric region at $(0, 0, 6 \text{ \AA})$. The qualocation results, denoted by solid lines with circles of varying sizes, are nearly indistinguishable except in the immediate vicinity of the charge in the high-dielectric region.

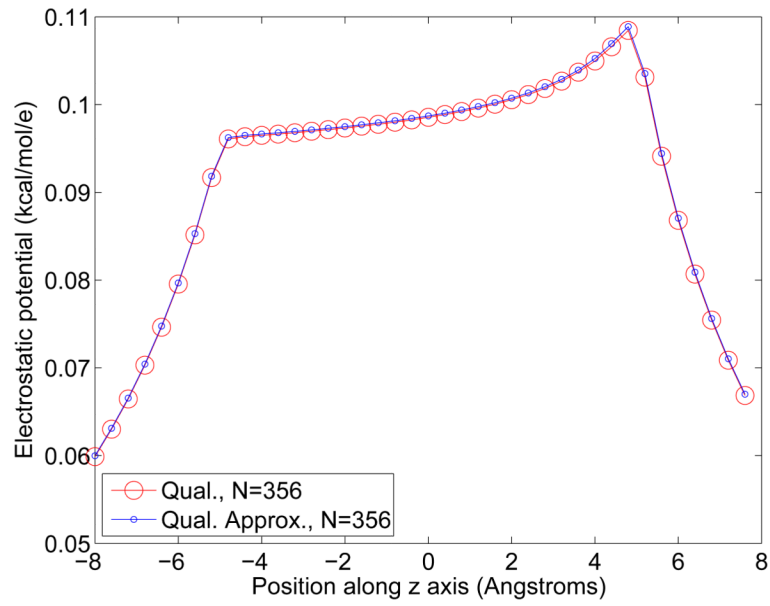


Figure 7. Accuracy of reaction potentials calculated when using exact and one-point-quadrature approaches to forming the entries of the right-hand-side in the qualocation method.